Engineering with Computers (2022) 38:111–127
https://doi.org/10.1007/s00366-020-01041-8

ORIGINAL ARTICLE

On model-based damage detection by an enhanced sensitivity function of modal flexibility and LSMR-Tikhonov method under incomplete noisy modal data

Hassan Sarmadi[1,2] · **Alireza Entezami**[1,3] · **Mansour Ghalehnovi**[1]

Received: 5 December 2019 / Accepted: 7 May 2020 / Published online: 25 May 2020
© Springer-Verlag London Ltd., part of Springer Nature 2020

Abstract

Sensitivity-based methods by the model updating strategy are still influential and reliable for structural damage detection. The major issue is to utilize a well-established sensitivity function that should be directly relevant to damage. Under noisy modal data, it is well known that the sensitivity-based model updating strategy is an ill-posed problem. The main aim of this article is to locate and quantify damage using incomplete noisy modal parameters by improving a sensitivity function of modal flexibility and proposing a new iterative regularization method for solving an ill-posed problem. The main contribution of the enhanced sensitivity formulation is to develop the derivative of eigenvalue and establish a more relevant sensitivity function to damage. The new regularization method is a combination of an iterative approach called least squares minimal residual and the well-known Tikhonov regularization technique. The key novel element of the proposed solution method is to choose an optimal regularization parameter during the iterative process rather than being required a prior. Numerical simulations are used to validate the accuracy and efficiency of the improved and proposed methods. Results demonstrate that the enhanced sensitivity function of the modal flexibility is more sensitive to damage in comparison with the basic formulation. Moreover, one can observe the robustness of the proposed solution method to solve the ill-posed problem for damage localization and quantification under noise-free and noisy modal data.

Keywords Damage detection · Sensitivity function · Modal flexibility · Noisy modal data · LSMR · Tikhonov regularization

1 Introduction

Structural damage detection is an important process in civil, mechanical and aerospace engineering systems, because adverse changes caused by damage in such systems lead to undesirable stresses and displacements, inappropriate dynamic behavior, adverse structural performance, failure and even collapse. Damage in a structure may emerge as material deterioration, geometric alterations, faults in boundary conditions, cracks, loose bolts and broken welds, corrosion, and fatigue. These may reduce the structural stiffness and result in adverse vibration responses. Therefore, there is a great necessity to assess the health and integrity of engineering systems for avoiding any irrecoverable events and decreasing the repair and rehabilitation costs.

To achieve these aims, structural health monitoring (SHM) provides a practical procedure by recording various structural responses (e.g. acceleration, strain, frequency domain data, modal data, etc.), evaluating structural state, and detecting any probable damage [1]. On this basis, an SHM system performs a damage detection process in four main steps: (1) early damage detection, (2) damage localization, (3) damage quantification, and (4) damage prognosis. The first step is a global process, which aims to perceive whether the damage is available throughout the structure. The damage localization and quantification steps are local

✉ Hassan Sarmadi
hassan.sarmadi@mail.um.ac.ir; sarmadi.ipesfp@gmail.com

1 Department of Civil Engineering, Faculty of Engineering, Ferdowsi University of Mashhad, P.O. Box 9177948974, Mashhad, Iran

2 Ideh Pardazan Etebar Sazeh Fanavar Pooya (IPESFP) Company, 29th Reza St Reza Blvd, P.O. Box 9176768544, Mashhad, Razavi Khorasan, Iran

3 Department of Civil and Environmental Engineering, Politecnico di Milano, Piazza L. da Vinci 32, 20133 Milan, Italy

procedures, which are intended to identify the damage location and quantify its severity. Eventually, the last step predicts the remaining lifetime of the structure, which is associated with the fields of fracture mechanics, fatigue-life analysis, and structural design assessment [2].

In general, model-based and data-based approaches are two kinds of SHM strategies for early damage detection, localization, and quantification. A model-based method relies on constructing a finite element (FE) model of the structure and utilizing a mathematical technique for the solution of the inverse problem of damage detection [3–7]. Most of the methods in this category are usually based on the concept of model updating [8, 9]. In contrast, a data-based approach uses raw measured vibration data and extracts features from them for SHM on the basis of statistical pattern recognition and machine learning [10–14].

Despite the popularity and applicability of data-based techniques, those are not sufficiently capable of quantifying the damage severity [15]. In contrast, model-based methods through the concept of model updating are still reliable and effective approaches to detecting, locating, and quantifying structural damage. A damage detection strategy based on the model updating relies on the modification of structural parameters by finding the differences between dynamic characteristics of the real structure and its finite element (FE) or analytical model. Under this theory, it is assumed that the FE model reflects a known or normal condition and the real structure or experimental model is an unknown (either undamaged or damaged) state [9]. Accordingly, the inherent structural properties and analytical vibration responses are simply obtained from the FE model, whereas the only experimental data are available from the real structure. Among all dynamic responses, the modal data (i.e., natural frequencies and mode shapes) are widely applied to the vibration-based damage detection methods. This is due to the fact that these parameters only depend on the inherent physical properties of the structure (i.e., mass, damping, and stiffness), regardless of the type of excitation.

Because the model updating process is an inverse problem and the relationship between the inherent structural parameters and modal data is intrinsically nonlinear, sensitivity-based methods are developed to simplify the solution of the inverse problem using the linearization of equations [16]. Most of the modal-based sensitivity functions rely upon taking the first-order derivative of the eigenvalue (the square of the natural frequency) and eigenvector (mode shape) with respect to the structural parameter based on the fundamental dynamic equations [16]. Although the measurement of modal frequencies is simpler and more accurate than the mode shapes, those are global dynamic characteristics and may not provide sufficient local information about damage [17]. This is because the damage is a local phenomenon and may not significantly affect the lower modes that are usually measured by modal testing [18]. Additionally, in order to acquire adequate modal displacements (mode shapes), it is necessary to equip the structure with a dense sensor network. This is a major limitation of the measurement and identification of mode shapes. Under such circumstances, an alternative way is to use modal flexibility that is a function of both the eigenvalues and eigenvectors. The salient feature of the modal flexibility is that it is more sensitive to damage than the modal frequencies and mode shapes [19]. As the other great merit, one can accurately estimate the modal flexibility matrix from only a few lower modes, because it is inversely proportional to the eigenvalues [20]. Due to such remarkable advantages, many researchers have utilized the change in the modal flexibility matrix as a damage index in vibration-based damage detection problems [21–24].

Taking all the merits of the modal flexibility into consideration, one of the important issues is how to define a well-established sensitivity function of the modal flexibility. General speaking, there are two approaches including: (1) the formulation of a sensitivity function based on the inverse of the stiffness matrix without using the modal data [25, 26] and (2) establishment of a sensitivity equation with the aid of the first-order derivatives of the eigenvalue and eigenvector [27]. Although the sensitivity formula of the first approach is very simple, it needs all modes, which may be impossible in most of the real applications. On this basis, it seems that the second approach provides a better and more beneficial sensitivity function for the modal flexibility. However, the major challenging issue in most of the sensitivity-based damage detection methods is to derive a well-established sensitivity function that should be sensitive to damage. In other words, this function should be related to the problem of damage detection and should provide sufficient damage detectability.

Another significant topic on the model-based damage detection is to solve an ill-posed inverse problem, which may arise from noisy modal data. This is a prominent issue, because a small perturbation caused by noise results in erroneous solutions. Regularization methods are usually used to solve ill-posed inverse problems [28–32]. In relation to damage detection, Weber et al. [33] utilized Tikhonov regularization and truncated singular value decomposition methods to solve a nonlinear model updating problem for damage identification in an iterative manner. Hou et al. [34] dealt with the problem of using the classical Tikhonov regularization technique for sparse damage identification by proposing l_1 regularization method. In connection with new regularization methods, Grip et al. [35] introduced total variation-based regularization as a well-established regularized solution approach to detect structural damage based on a sensitivity-based model updating strategy. Entezami et al. [3] proposed regularized least squares minimal residual method to solve an ill-posed inverse problem regarding the sensitivity-based damage detection under a highly ill-conditioned sensitivity matrix and noise measurements. Despite reasonable researches about the model-based damage detection via regularization methods, the ill-posedness is still an open problem, particularly choosing an optimal regularization value.

The main objective of this article is to locate and quantify structural damage using incomplete noisy modal data. For these purposes, an improved sensitivity function of the modal flexibility is proposed to establish a more sensitive formulation to damage. The improvement relies on the development of the derivative of eigenvalue, which is directly used in the general formulation of the sensitivity of the modal flexibility. In order to address the incompleteness of mode shapes, system equivalent reduction expansion process (SEREP) approach is applied to expand the measured modal displacements. A new regularized solution method as the combination of least squares minimal residual (LSMR) and the well-known Tikhonov regularization is proposed to solve the ill-posed inverse problem of damage detection under noisy conditions. The main contribution of the proposed solution method called *LSMR-Tikhonov* is to select an optimal regularization parameter during the iterative process rather than being required a prior. The accuracy and performance of the enhanced sensitivity function and proposed solution method are verified by two numerical models. A statistical threshold limit is also incorporated to increase the reliability of damage localization. Results show that the methods presented here are precisely able to locate and quantify single and multiple damage cases, even under noisy modal data. Moreover, it is observed that the enhanced sensitivity function of the modal flexibility is more sensitive to damage compared to the basic formulation.

2 Enhanced sensitivity function of modal flexibility

The modal flexibility $\mathbf{F}$ is a function of the eigenvalues and eigenvectors. This function generally represents a static deflection profile caused by a unit load [27]. For a structural system with n degrees-of-freedom (DOFs), the function of modal flexibility is defined as:

$$\mathbf{F} = \sum_{i=1}^{n} \frac{1}{\lambda_i} \boldsymbol{\varphi}_i \boldsymbol{\varphi}_i^T \tag{1}$$

where λ_i and $\boldsymbol{\varphi}_i$ represent the ith eigenvalue (the square of natural frequency) and eigenvector (mode shape) of the FE model of the structural system. These modal parameters are derived from the analytical mass and stiffness matrices; that is, $\mathbf{M}, \mathbf{K} \in \mathfrak{R}^{n\times n}$. One should clarify here that it is not always feasible to measure all the modal data of the real structure due to some practical and economic limitations. Furthermore, one cannot measure all modal displacements at all DOFs. In such cases, the measured modal frequencies and mode shapes are incomplete in the sense that those are only available and measurable in a few modes and DOFs [3]. To address the incompleteness of mode shapes, it is possible to apply the SEREP technique [36] so as to expand them and obtain the analytical and experimental modal displacements with the same dimensions. On another important note, the basic requirement of a model-based method is that both the analytical and measured (experimental) mode shapes should be scaled [16]. Due to the availability of the mass matrix of the FE model, the analytical mode shapes are mass normalized. However, the inherent properties of the real structure are often unknown. Therefore, the measured modal displacements need to be normalized. An effective way for this issue is to apply the mode scale factor [3].

With these descriptions, the modal flexibility matrix of the real or experimental model is derived from truncated lower modes of the modal frequencies and mode shapes. Considering the only m measured modes, the modal flexibility matrix ($\hat{\mathbf{F}}$) regarding the real structure is written as follows:

$$\hat{\mathbf{F}} = \sum_{i=1}^{m} \frac{1}{\hat{\lambda}_i} \hat{\boldsymbol{\varphi}}_i \hat{\boldsymbol{\varphi}}_i^T \tag{2}$$

where $\hat{\lambda}_i$ and $\hat{\boldsymbol{\varphi}}_i$ stand for the ith measured modal frequency and normalized mode shape vector, which has been scaled and completed by the mode scale factor and the SEREP technique, respectively. An interesting characteristic of $\mathbf{F}$ and $\hat{\mathbf{F}}$ is that both of them produce n-by-n square matrices in spite of using the incomplete modal data. Most of the sensitivity functions originate from the first-order derivative of dynamic characteristics with respect to the structural parameter of the undamaged state. Accordingly, the general sensitivity formulation for the ith mode is given by:

$$\frac{\partial \mathbf{F}_i}{\partial p} = -\frac{1}{\lambda_i^2} \frac{\partial \lambda_i}{\partial p} \boldsymbol{\varphi}_i \boldsymbol{\varphi}_i^T + \frac{1}{\lambda_i} \frac{\partial \boldsymbol{\varphi}_i}{\partial p} \boldsymbol{\varphi}_i^T + \frac{1}{\lambda_i} \boldsymbol{\varphi}_i \frac{\partial \boldsymbol{\varphi}_i^T}{\partial p} \tag{3}$$

It is better to arrange Eq. (3) in the following form:

$$\frac{\partial \mathbf{F}_i}{\partial p} = -\frac{1}{\lambda_i^2} \frac{\partial \lambda_i}{\partial p} \boldsymbol{\varphi}_i \boldsymbol{\varphi}_i^T + \frac{1}{\lambda_i} \left(\frac{\partial \boldsymbol{\varphi}_i}{\partial p} \boldsymbol{\varphi}_i^T + \left(\frac{\partial \boldsymbol{\varphi}_i}{\partial p} \boldsymbol{\varphi}_i^T \right)^T \right) \tag{4}$$

As the above equation appears, the main components of the sensitivity function are the first-order derivatives (sensitivities) of the eigenvalue and eigenvector. Based on the eigenvalue problem, the sensitivity of eigenvector is given by:

$$\left(\mathbf{K} - \lambda_i \mathbf{M} \right) \frac{\partial \boldsymbol{\varphi}_i}{\partial p} = \frac{\partial \lambda_i}{\partial p} \mathbf{M} \boldsymbol{\varphi}_i - \frac{\partial \mathbf{K}}{\partial p} \boldsymbol{\varphi}_i \tag{5}$$

For the problem of damage detection, it is possible to neglect the derivative of mass matrix since the damage usually does not affect this structural property and it often remains invariant. Let $\mathbf{L}$ denotes the inverse of $\mathbf{K}-\lambda_i\mathbf{M}$. Rather than using the classical inverse operator, which may lead to an inaccurate inversion in the case of an ill-conditioned matrix, it is better to utilize the pseudo-inverse procedure based on singular value decomposition (SVD) [37]. For this purpose, the matrix $\mathbf{K}$-$\lambda_i\mathbf{M}$ is decomposed into three matrices in the following form:

$$\left(\mathbf{K}-\lambda_i\mathbf{M}\right)=\mathbf{A}\boldsymbol{\Sigma}\mathbf{B}^T \tag{6}$$

in which $\boldsymbol{\Sigma}$ is a diagonal matrix. Thus:

$$\mathbf{L}=\mathbf{B}\boldsymbol{\Sigma}^{+}\mathbf{A}^T \tag{7}$$

where "+" denotes the pseudo-inverse. Therefore, the derivative of mode shape is modified as:

$$\frac{\partial\boldsymbol{\varphi}_i}{\partial p}=\mathbf{L}\frac{\partial\lambda_i}{\partial p}\mathbf{M}\boldsymbol{\varphi}_i-\mathbf{L}\frac{\partial\mathbf{K}}{\partial p}\boldsymbol{\varphi}_i \tag{8}$$

Substituting Eq. (8) into Eq. (4) yields:

$$\frac{\partial\mathbf{F}_i}{\partial p}=-\frac{1}{\lambda_i^2}\frac{\partial\lambda_i}{\partial p}\boldsymbol{\Psi}_i+\frac{\mathbf{L}}{\lambda_i}\left(\frac{\partial\lambda_i}{\partial p}\mathbf{M}-\frac{\partial\mathbf{K}}{\partial p}\right)\boldsymbol{\Psi}_i+\left(\frac{\mathbf{L}}{\lambda_i}\left(\frac{\partial\lambda_i}{\partial p}\mathbf{M}-\frac{\partial\mathbf{K}}{\partial p}\right)\boldsymbol{\Psi}_i\right)^T \tag{9}$$

where $\boldsymbol{\Psi}_i=\boldsymbol{\varphi}_i\boldsymbol{\varphi}_i^{\mathrm{T}}\in\Re^{n\times n}$. Unlike $\partial\mathbf{K}/\partial p$, the first-order derivative of the eigenvalue is unknown and should be determined. An efficient and well-known approach to determining the derivative of eigenvalue is the method of Fox and Kapoor [38]:

$$\frac{\partial\lambda_i}{\partial p}=\boldsymbol{\varphi}_i^T\left(\frac{\partial\mathbf{K}}{\partial p}-\lambda_i\frac{\partial\mathbf{M}}{\partial p}\right)\boldsymbol{\varphi}_i \tag{10}$$

For the problem of damage detection, this equation can be rewritten as:

$$\frac{\partial\lambda_i}{\partial p}=\boldsymbol{\varphi}_i^T\frac{\partial\mathbf{K}}{\partial p}\boldsymbol{\varphi}_i \tag{11}$$

Although Fox and Kapoor's method is broadly applied to the problem of damage detection, one can develop it to establish a more robust sensitivity function pertinent to damage. Using the stiffness-orthogonality condition, $\partial\lambda_i/\partial p$ can be formulated as follows:

$$\frac{\partial\lambda_i}{\partial p}=\left(\frac{\partial\boldsymbol{\varphi}_i^T}{\partial p}\right)\mathbf{K}\boldsymbol{\varphi}_i+\boldsymbol{\varphi}_i^T\frac{\partial\mathbf{K}}{\partial p}\boldsymbol{\varphi}_i+\boldsymbol{\varphi}_i^T\mathbf{K}\frac{\partial\boldsymbol{\varphi}_i}{\partial p} \tag{12}$$

The stiffness matrix is symmetric, and therefore, it is reasonable that $\mathbf{K}\boldsymbol{\varphi}_i=\boldsymbol{\varphi}_i^{\mathrm{T}}\mathbf{K}$. Hence, the above equation is modified as:

$$\frac{\partial\lambda_i}{\partial p}=\boldsymbol{\varphi}_i^T\frac{\partial\mathbf{K}}{\partial p}\boldsymbol{\varphi}_i+2\boldsymbol{\varphi}_i^T\mathbf{K}\frac{\partial\boldsymbol{\varphi}_i}{\partial p} \tag{13}$$

However, the first term of this equation describes the variation of the stiffness matrix as the main damage index, one can approximate the derivative of mode shape in the second term of Eq. (13) based on the rate of change in the stiffness matrix as follows [18]:

$$\frac{\partial\boldsymbol{\varphi}_i}{\partial p}\cong\sum_{r=1}^{m}\frac{1}{\lambda_i-\lambda_r}\boldsymbol{\varphi}_r^T\frac{\partial\mathbf{K}}{\partial p}\boldsymbol{\varphi}_i\boldsymbol{\varphi}_r \tag{14}$$

Therefore, the first-order derivative of the eigenvalue is improved as:

$$\frac{\partial\lambda_i}{\partial p}=\boldsymbol{\varphi}_i^T\frac{\partial\mathbf{K}}{\partial p}\boldsymbol{\varphi}_i+2\boldsymbol{\varphi}_i^T\mathbf{K}\sum_{r=1}^{m}\frac{1}{\lambda_i-\lambda_r}\boldsymbol{\varphi}_r^T\frac{\partial\mathbf{K}}{\partial p}\boldsymbol{\varphi}_i\boldsymbol{\varphi}_r \tag{15}$$

Assume that:

$$\xi=2\boldsymbol{\varphi}_i^T\mathbf{K}\left(\sum_{r=1}^{m}\frac{1}{\lambda_i-\lambda_r}\boldsymbol{\varphi}_r^T\frac{\partial\mathbf{K}}{\partial p}\boldsymbol{\varphi}_i\boldsymbol{\varphi}_r\right) \tag{16}$$

By inserting Eq. (15) into Eq. (9), the enhanced sensitivity function of the modal flexibility for the ith mode is proposed as:

$$\frac{\partial\mathbf{F}_i}{\partial p}=-\frac{1}{\lambda_i^2}\left(\boldsymbol{\varphi}_i^T\frac{\partial\mathbf{K}}{\partial p}\boldsymbol{\varphi}_i+\xi\right)\boldsymbol{\Psi}_i+\frac{\mathbf{L}}{\lambda_i}\left(\left(\boldsymbol{\varphi}_i^T\frac{\partial\mathbf{K}}{\partial p}\boldsymbol{\varphi}_i+\xi\right)\mathbf{M}-\frac{\partial\mathbf{K}}{\partial p}\right)\boldsymbol{\Psi}_i+\left(\frac{\mathbf{L}}{\lambda_i}\left(\left(\boldsymbol{\varphi}_i^T\frac{\partial\mathbf{K}}{\partial p}\boldsymbol{\varphi}_i+\xi\right)\mathbf{M}-\frac{\partial\mathbf{K}}{\partial p}\right)\boldsymbol{\Psi}_i\right)^T \tag{17}$$

which can be arranged as follows:

$$\frac{\partial\mathbf{F}_i}{\partial p}=\frac{\mathbf{L}}{\lambda_i}\left(\boldsymbol{\varphi}_i^T\frac{\partial\mathbf{K}}{\partial p}\boldsymbol{\varphi}_i\mathbf{M}+\xi\mathbf{M}-\frac{\partial\mathbf{K}}{\partial p}\right)\boldsymbol{\Psi}_i-\frac{1}{\lambda_i^2}\left(\boldsymbol{\varphi}_i^T\frac{\partial\mathbf{K}}{\partial p}\boldsymbol{\varphi}_i+\xi\right)\boldsymbol{\Psi}_i+\left(\frac{\mathbf{L}}{\lambda_i}\left(\boldsymbol{\varphi}_i^T\frac{\partial\mathbf{K}}{\partial p}\boldsymbol{\varphi}_i\mathbf{M}+\xi\mathbf{M}-\frac{\partial\mathbf{K}}{\partial p}\right)\boldsymbol{\Psi}_i\right)^T \tag{18}$$

For all measured modes, the enhanced sensitivity function is then formulated in the following form:

$$\frac{\partial\mathbf{F}}{\partial p}=\sum_{i=1}^{m}\frac{\partial\mathbf{F}_i}{\partial p} \tag{19}$$

The major improvement in the new sensitivity formulation of the modal flexibility directly relies on the development of the sensitivity of eigenvalue by adding the expression ξ. In other words, one can obtain the basic formulation of the modal flexibility by eliminating this expression.

3 Damage detection strategy

A perturbation of each structural parameter will lead to changes in the structural stiffness and modal flexibility. Based on the first-order Taylor's series, the changes are described as:

$$\Delta\mathbf{F} = \sum_{j=1}^{ne} \frac{\partial \mathbf{F}}{\partial p_j} \Delta p_j \tag{20}$$

$$\Delta\mathbf{K} = \sum_{j=1}^{ne} \frac{\partial \mathbf{K}_j}{\partial p_j} \Delta p_j \tag{21}$$

where ne and $\mathbf{K}_j$ denote the number of elements of the FE model and the local stiffness matrix of the jth element, respectively. By replacing Eq. (18) into Eq. (20) and using the expression of the stiffness discrepancy function presented in Eq. (21), the discrepancy matrix of the modal flexibility is given by:

$$\Delta\mathbf{F}= \sum_{i=1}^{m} \left(\frac{\mathbf{L}}{\lambda_i} (\boldsymbol{\varphi}_i^T \Delta\mathbf{K} \boldsymbol{\varphi}_i \mathbf{M} + \xi \mathbf{M} - \Delta\mathbf{K}) \boldsymbol{\Psi}_i - \frac{1}{\lambda_i^2} (\boldsymbol{\varphi}_i^T \Delta\mathbf{K} \boldsymbol{\varphi}_i + \xi) \boldsymbol{\Psi}_i + \left(\frac{\mathbf{L}}{\lambda_i} (\boldsymbol{\varphi}_i^T \Delta\mathbf{K} \boldsymbol{\varphi}_i \mathbf{M} + \xi \mathbf{M} - \Delta\mathbf{K}) \boldsymbol{\Psi}_i \right)^T \right) \tag{22}$$

where ξ should be modified as:

$$\xi = 2\boldsymbol{\varphi}_i^T \mathbf{K} \left(\sum_{r=1}^{m} \frac{1}{\lambda_i - \lambda_r} \boldsymbol{\varphi}_r^T \Delta\mathbf{K} \boldsymbol{\varphi}_i \boldsymbol{\varphi}_r \right) \tag{23}$$

Since $\Delta\mathbf{K} = \mathbf{K} - \hat{\mathbf{K}}$ and the stiffness of the damaged (real) structure ($\hat{\mathbf{K}}$) are unknown, the stiffness discrepancy matrix can be rewritten as follows [27]:

$$\Delta\mathbf{K} = \sum_{j=1}^{ne} \nu_j \mathbf{K}_j \tag{24}$$

where ν_j is the stiffness reduction factor of the jth element. It is important to point out that $\nu_j \in [0\ 1]$, in which zero is indicative of the undamaged condition and one ideally represents the damaged state as the entire loss of the element stiffness. Thus, the discrepancy modal flexibility matrix of Eq. (22) can be expressed in the following form:

$$\Delta\mathbf{F} = \sum_{j=1}^{ne} \nu_j \boldsymbol{\Gamma}_j \tag{25}$$

where

$$\boldsymbol{\Gamma}_j = \sum_{i=1}^{m} \left(\frac{\mathbf{L}}{\lambda_i} (\boldsymbol{\varphi}_i^T \mathbf{K}_j \boldsymbol{\varphi}_i \mathbf{M} + \xi \mathbf{M} - \mathbf{K}_j) \boldsymbol{\Psi}_i - \frac{1}{\lambda_i^2} (\boldsymbol{\varphi}_i^T \mathbf{K}_j \boldsymbol{\varphi}_i + \xi) \boldsymbol{\Psi}_i + \left(\frac{\mathbf{L}}{\lambda_i} (\boldsymbol{\varphi}_i^T \mathbf{K}_j \boldsymbol{\varphi}_i \mathbf{M} + \xi \mathbf{M} - \mathbf{K}_j) \boldsymbol{\Psi}_i \right)^T \right) \tag{26}$$

Note that $\mathbf{K}_j$ should be replaced with $\Delta\mathbf{K}$ for the expression of ξ in Eq. (23). Expanding Eq. (25), one yields:

$$\Delta\mathbf{F} = \boldsymbol{\Gamma}_1 a_1 + \boldsymbol{\Gamma}_2 a_2 + \cdots + \boldsymbol{\Gamma}_{ne} a_{ne} \tag{27}$$

For the process of damage detection, this expression can be changed into a linear inverse problem as:

$$[\mathbf{S}]\{\mathbf{a}\} = \{\Delta\mathbf{f}\} \tag{28}$$

where $\mathbf{S} \in \Re^{n^2 \times ne}$ ($n^2 \gg ne$), $\mathbf{a} \in \Re^{ne}$, and $\Delta\mathbf{f} \in \Re^{n^2}$. More precisely, one can expand Eq. (28) as follows:

$$\begin{bmatrix} \mathbf{s}_1 & \cdots & \mathbf{s}_j & \cdots & \mathbf{s}_{ne} \end{bmatrix} \begin{Bmatrix} a_1 \\ \vdots \\ a_j \\ \vdots \\ a_{ne} \end{Bmatrix} = \begin{Bmatrix} \Delta\mathbf{f}_1 \\ \vdots \\ \Delta\mathbf{f}_i \\ \vdots \\ \Delta\mathbf{f}_{n^2} \end{Bmatrix} \tag{29}$$

where $\mathbf{s}_j \in \Re^{n^2}$ is the jth vector of the matrix $\boldsymbol{\Gamma}$ based on the process of linear matrix vectorization. Furthermore, $\Delta\mathbf{f}_i$ represents the ith row of the modal flexibility discrepancy matrix.

4 LSMR-Tikhonov method

4.1 General concepts

The process of damage detection based on the model updating strategy is an inverse problem, which may be ill-posed. In general, a well-posed problem has three main conditions including existence, uniqueness, and stability. If the problem fails to satisfy any of these conditions, it is ill-posed [28]. The existence and uniqueness are often assured by introducing additional assumptions, which lead to some generalized solutions to the problem. The solution stability depends on the perturbation in measurements such as the availability of noise in the modal data. In such cases, the solution to the linear inverse problem such as Eq. (28) becomes unstable even when it exists and to be unique. To alleviate this limitation, regularization methods are usually used to achieve the stabilization of the ill-posed inverse problems.

The regularized solution to Eq. (28) based on the Tikhonov regularization technique relies on an estimation of $\mathbf{a}_{\text{true}}$ from the least squares (LS) problem as follows:

$$\min_{\mathbf{a}} \|\mathbf{S}.\mathbf{a} - \Delta\mathbf{f}\|_2^2 + \gamma^2\|\mathbf{a}\|_2^2 \tag{30}$$

where the regularization parameter γ controls the smoothness of the solution. The main limitation of the Tikhonov regularization technique is to select an appropriate regularization parameter. Furthermore, this regularized solution method falls into a direct approach, which solves the ill-posed inverse problem once. As an alternative, it is possible to exploit iterative regularization techniques for solving the LS problem in the following form:

$$\min_{\mathbf{a}} \|\mathbf{S}.\mathbf{a} - \Delta\mathbf{f}\|_2 \tag{31}$$

The major objective of iterative regularization methods is to approximate solution $\mathbf{a}_k$ after k iterations. It is well known that iterative approaches indicate semi-convergence on the ill-posed problem [39]. In addition, the choice of a proper stopping condition for the termination of the iterative process is an important and nontrivial task. Considering these limitations, hybrid methods are efficiently used to deal with the semi-convergence treatment in most of the iterative techniques and avoid choosing a regularization parameter a prior, which is a crucial requirement for all regularization methods. The central idea behind a hybrid method is to utilize an iterative algorithm to project the original ill-posed LS problem onto Krylov subspaces and then apply a direct regularization technique to solve the relatively small projected LS problem. The regularization of the projected problem at each iteration affects stabilizing the convergence behavior, which leads to reducing the risk of computing a poor solution. Recently, a new hybrid method has been proposed by Chung and Palmer [39] to solve the ill-posed inverse problem through the combination of LSMR and Tikhonov regularization. This method, which is called here LSMR-Tikhonov, is applied to solve Eq. (28) for damage localization and quantification.

4.2 Solution algorithm

The LSMR method is an iterative solver of the LS equation and uses the Golub–Kahan (GK) bidiagonalization process to generate a Krylov subspace. The application of this iterative solution method to the vibration-based problem can be found in Sarmadi et al. [9]. Similar to the other iterative algorithms under the Krylov subspace theory, the LSMR-Tikhonov method is based on the GK bidiagonalization process. Generally, this process is a critical and essential part of each iterative algorithm. Given the matrix $\mathbf{S}$ and vector $\Delta\mathbf{f}$, the GK bidiagonalization is an iterative procedure to transform matrix $[\Delta\mathbf{f}\ \mathbf{S}]$ to upper-bidiagonal form $[\beta_1\mathbf{e}_1\ \mathbf{B}_k]$. Note that the vector $\mathbf{e}$ is a column of an identity matrix. With initialization $\beta_1 = \|\Delta\mathbf{f}\|_2$, $\mathbf{u}_1 = \Delta\mathbf{f}/\beta_1$, and $\alpha_1\mathbf{v}_1 = \mathbf{S}^{\mathrm{T}}\mathbf{u}_1$, the k^{th} iteration of the GK process calculates orthogonal vector $\mathbf{u}_{k+1}$ and $\mathbf{v}_{k+1}$ such that:

$$\begin{aligned} \beta_{k+1}\mathbf{u}_{k+1} &= \mathbf{S}\mathbf{v}_k - \alpha_k\mathbf{u}_k \\ \alpha_{k+1}\mathbf{v}_{k+1} &= \mathbf{S}^T\mathbf{u}_{k+1} - \beta_{k+1}\mathbf{v}_k \end{aligned} \tag{32}$$

After k steps, one can obtain:

$$\mathbf{V}_k = \begin{bmatrix} \mathbf{v}_1 & \cdots & \mathbf{v}_k \end{bmatrix} \tag{33}$$

$$\mathbf{U}_k = \begin{bmatrix} \mathbf{u}_1 & \cdots & \mathbf{u}_k \end{bmatrix} \tag{34}$$

$$\mathbf{B}_k = \begin{bmatrix} \alpha_1 & & & \\ \beta_1 & \alpha_2 & & \\ & \beta_2 & \ddots & \\ & \ddots & \ddots & \alpha_k \\ & & & \beta_{k+1} \end{bmatrix} \tag{35}$$

where $\mathbf{V}_k \in \Re^{n\times k}$, $\mathbf{U}_k \in \Re^{n^2\times k}$, and $\mathbf{B}_k \in \Re^{(k+1)\times k}$. Under such conditions, one can write:

$$\mathbf{S}\mathbf{V}_k = \mathbf{U}_{k+1}\mathbf{B}_k \tag{36}$$

$$\mathbf{S}^T\mathbf{U}_{k+1} = \mathbf{V}_{k+1}\mathbf{H}_{k+1}^T \tag{37}$$

in which $\mathbf{H}_{k+1} = [\mathbf{B}_k\ \alpha_{k+1}\mathbf{e}_{k+1}] \in \Re^{(k+1)\times(k+1)}$. For the algorithm of the LSMR method, an unknown vector $\mathbf{y}_k$ is chosen at each iteration to minimize $\|\mathbf{S}^{\mathrm{T}}\mathbf{r}_k\|$, where $\mathbf{r}_k = \mathbf{S}.\mathbf{a}_k - \Delta\mathbf{f}$ is the residual vector. In other words, $\mathbf{y}_k$ is the solution to the following sub-problem:

$$\min_{\mathbf{a}} \left\|\mathbf{S}^T(\mathbf{S}\mathbf{a} - \Delta\mathbf{f})\right\|_2 = \min_{\mathbf{y}} \left\| \begin{pmatrix} \mathbf{B}_k^T\mathbf{B}_k \\ \bar{\beta}_{k+1}\mathbf{e}_k^T \end{pmatrix} \mathbf{y} - \bar{\beta}_1\mathbf{e}_1 \right\|_2 = \min_{\mathbf{y}} \left\|\hat{\mathbf{B}}_k\mathbf{y} - \bar{\beta}_1\mathbf{e}_1\right\|_2 \tag{38}$$

where $\bar{\beta}_l = \alpha_l\beta_l$ and $l = 1, k+1$. Once the vector $\mathbf{y}_k$ has been determined, the final solution corresponds to $\mathbf{a}_k = \mathbf{V}_k\mathbf{y}_k$. Since LSMR suffers from the semi-convergence behavior and $\hat{\mathbf{B}}_k$ becomes ill-conditioned in large GK iterations, it is preferable to solve Eq. (38) by the Tikhonov regularization technique as follows:

$$\mathbf{y}_k = \arg\min_{\mathbf{y}} \left\|\hat{\mathbf{B}}_k\mathbf{y} - \bar{\beta}_1\mathbf{e}_1\right\|_2^2 + \gamma^2\|\mathbf{y}\|_2^2 \tag{39}$$

Based on the standard form of Tikhonov regularization, which is given by,

$$\min_{\mathbf{a}} \left\| \begin{pmatrix} \mathbf{S} \\ \gamma \mathbf{I} \end{pmatrix} \mathbf{a} - \begin{pmatrix} \Delta \mathbf{f} \\ 0 \end{pmatrix} \right\|_2^2 \tag{40}$$

Equation (39) can be rewritten as follows:

$$\mathbf{y}_k = \arg\min_{\mathbf{y}} \left\| \bar{\mathbf{S}}^T \bar{\mathbf{r}}_k \right\|_2 = \arg\min_{\mathbf{y}} \left\| \hat{\mathbf{B}}_k \mathbf{y} - \bar{\beta}_1 \mathbf{e}_1 + \gamma^2 \begin{pmatrix} \mathbf{y} \\ 0 \end{pmatrix} \right\|_2 \tag{41}$$

where $\bar{\mathbf{r}}_k = \Delta\bar{\mathbf{f}} - \bar{\mathbf{S}}\mathbf{a}_k$, $\bar{\mathbf{S}} = \begin{pmatrix} \mathbf{S} \\ \gamma \mathbf{I} \end{pmatrix}$, and $\Delta\bar{\mathbf{f}} = \begin{pmatrix} \Delta \mathbf{f} \\ 0 \end{pmatrix}$.

4.3 Regularization parameter

The critical step of solving the ill-posed LS problem is to choose an appropriate regularization parameter. Since $\hat{\mathbf{B}}_k$ may be small for small values of k, it is possible to utilize methods based on SVD for determining γ. In this article, the well-known generalized cross-validation (GCV) is used to choose an appropriate regularization parameter. The general function of GCV is given by:

$$G(\gamma) = \frac{ne \left\| \Delta \mathbf{f} - \mathbf{S}\mathbf{a}_\gamma \right\|_2^2}{\left(trace\left(\mathbf{I} - \mathbf{S}\mathbf{S}_\gamma^\dagger \right) \right)^2} \tag{42}$$

where $\mathbf{S}_\gamma^\dagger = (\mathbf{S}^T\mathbf{S} + \gamma^2\mathbf{I})^{-1}\mathbf{S}^T$ and $\mathbf{I}$ is an identity matrix. For this formulation, the optimal regularization parameter is chosen to minimize the GCV function. Although Eq. (42) is a widely accepted formulation, it is not suitable to use in the LSMR-Tikhonov method. As an alternative, a proper regularization parameter is selected at each iteration to minimize a new GCV function. For this aim, $\hat{\mathbf{B}}_k$ is initially decomposed into three sub-matrices based on the SVD technique as:

$$\hat{\mathbf{B}}_k = \hat{\mathbf{P}}_k \begin{pmatrix} \hat{\mathbf{Z}}_k \\ 0 \end{pmatrix} \hat{\mathbf{Q}}_k^T \tag{43}$$

Thus, the new GCV function associated with the LSMR-Tikhonov method is expressed as:

$$\hat{G}(\gamma_k) = \frac{k\bar{\beta}_1^2 \left(\sum_{i=1}^k \left(\frac{\gamma^2}{\sigma_i^2+\gamma^2} \left\{ \hat{\mathbf{P}}_k^T \mathbf{e}_1 \right\}_i \right)^2 + \left(\left\{ \hat{\mathbf{P}}_k^T \mathbf{e}_1 \right\}_{k+1} \right)^2 \right)}{\left(1 + \sum_{i=1}^k \frac{\gamma^2}{\sigma_i^2+\gamma^2} \right)^2} \tag{44}$$

where σ_i is the ith diagonal element of $\hat{\mathbf{Z}}_k$. Based on Eq. (44), the regularization parameter at the kth iteration is chosen as the optimal value [39].

4.4 Stopping criterion

Another significant issue in the LSMR-Tikhonov method is to determine a stopping condition for terminating the iteration for the GK process. In addition, this condition plays a prominent role in determining the optimal regularization parameter at the kth iteration, where k is directly obtained from the stopping criterion. Since standard techniques for defining the stopping condition were not developed with ill-posed inverse problems, a GCV function is introduced in the LSMR-Tikhonov method. Consider the following problem:

$$\min_{\mathbf{a}} \left\| \mathbf{S}^T\mathbf{S}\mathbf{a} - \mathbf{S}^T \Delta \mathbf{f} \right\|_2 \tag{45}$$

On this basis, the GCV function for determining a stopping condition (k) can be expressed as:

$$\bar{G}(k) = \frac{ne \left\| (\mathbf{I} - \mathbf{S}^T\mathbf{S}\mathbf{X}_\gamma)\mathbf{S}^T \Delta \mathbf{f} \right\|_2^2}{\left(trace(\mathbf{I} - \mathbf{S}^T\mathbf{S}\mathbf{X}_\gamma) \right)^2} \tag{46}$$

in which

$$\mathbf{X}_\gamma = \mathbf{V}_k \left(\hat{\mathbf{B}}_k^T \hat{\mathbf{B}}_k + \gamma_k^2 \mathbf{I} \right)^{-1} \hat{\mathbf{B}}_k^T \mathbf{V}_{k+1}^T \tag{47}$$

Using the SVD of $\hat{\mathbf{B}}_k$, Eq. (46) can be simplified as:

$$\bar{G}(k) = \frac{ne\, \bar{\beta}_1^2 \left(\sum_{i=1}^k \left(\frac{\gamma^2}{\sigma_i^2+\gamma^2} \left\{ \hat{\mathbf{P}}_k^T \mathbf{e}_1 \right\}_i \right)^2 + \left(\left\{ \hat{\mathbf{P}}_k^T \mathbf{e}_1 \right\}_{k+1} \right)^2 \right)}{\left(ne - \sum_{i=1}^k \frac{\sigma_i^2}{\sigma_i^2+\gamma^2} \right)^2} \tag{48}$$

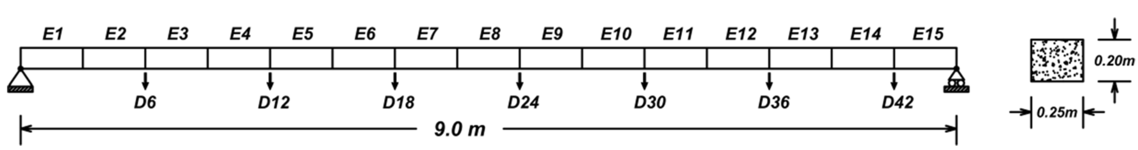

Fig. 1 The simply supported beam (*E: Element and D: Degree-of-freedom*)

Table 1 Damage cases for the simply supported beam

Case no.	Label	Damage location	Damage severity (%)
1	DC1	E8	20
2	DC2	E8	50
3	DC3	E5	10
		E15	20
4	DC4	E5	30
		E15	40

Based on the above expression, the number of iterations (k) in the LSMR-Tikhonov method is a value when $\bar{G}(k)$ becomes minimum.

5 Numerical examples

5.1 A simply supported beam

In the first numerical example, the accuracy and efficiency of the enhanced and proposed methods are verified by a simply supported beam as shown in Fig. 1. This beam is constructed from 15 elements (E1-E15) with a total of 45 DOFs. Each element has 0.25 m width, 0.20 m height, and 0.6 m length. The modulus of elasticity and material density are identical to 28 GPa and 2500 kg/m^3, respectively. Using a two-dimensional beam element, the FE model of the beam (i.e., the mass and stiffness matrices) is obtained by in-house MATLAB codes. Several damage scenarios are defined by decreasing the stiffness of some elements. Table 1 presents the information about the type, location, and severity of damages. Note that the FE model and some damage cases of this numerical model are based on [27].

Based on the model updating strategy for the damage detection problem, the initial FE model of the beam is chosen as the undamaged or known structural state. In this regard, the full sets of analytical modal parameters are obtained by the eigenvalue problem. Applying the stiffness reduction factors as the sources of damage severities, the modal data of the damaged conditions are determined as well. In order to simulate a realistic condition, the first five natural frequencies along with the modal displacements at D6, D12, D18, D24, D30, D36, and D42 are only utilized to consider the incompleteness conditions of the measured modal data in the damaged states. As another practical issue, some noise levels are imposed on the measured modal parameters to simulate noisy measurements. For the numerical problems, the noisy modal frequency and mode shape are simply simulated as:

$$\hat{\boldsymbol{\varphi}}_i^* = \hat{\boldsymbol{\varphi}}_i + \eta\,\mathbf{w_n} \tag{49}$$

$$\hat{\lambda}_i^* = \hat{\lambda}_i + \eta\,w_n \tag{50}$$

where η denotes the noise level; $\mathbf{w_n}$ is a randomly normal distribution vector and w_n represents a random scalar value. For the simply supported beam, 0%, 5%, and 20% noise levels are considered. It is important to mention that the mass matrix of the analytical beam model (the undamaged condition) is available. Hence, the analytical mode shapes are mass normalized. In this regard, the incomplete measured modal displacements of the beam in the damaged states are normalized by the mode scale factor [3]. Furthermore, the SEREP technique is utilized to expand the mass-normalized measured mode shapes. Applying the obtained information of the undamaged and damaged conditions, the LSMR-Tikhonov method is used to solve the ill-posed LS problem presented in Eq. (28). In addition, a threshold limit is incorporated to increase the reliability of damage localization results. From a statistical viewpoint, this limit is identical to a 95% confidence interval of the damaged vector (**a**). For the sake of convenience, the threshold limit is defined as:

$$\tau = \mu_a + 1.96\left(\frac{\sigma_a}{\sqrt{ne}}\right) \tag{51}$$

where μ_a and σ_a represent the mean and standard deviation of the damage vector. On this basis, each quantity of **a** that exceeds the threshold limit is indicative of the location of damage. Note that the absolute quantities of the damage vector ($|\mathbf{a}|$) should be allocated to determine the threshold limit. Table 2 presents the number of iterations for the solution of the damage equation by the LSMR-Tikhonov method. It should be pointed out that the LSMR method is utilized to solve the LS problem in the zero noise level (the noise-free modal data). For the other noise levels, the number of iterations needed to the LSMR-Tikhonov method is obtained from $\bar{G}(k)$. Figures 2 and 3 show the regularization parameters gained by the GCV function $\hat{G}(\gamma_k)$ for the only noisy modal data. In these figures, the optimal regularization parameter in each plot is observable at the last iteration as can be detectable by the red circle.

Table 2 The number of iterations for the LSMR (0% noise level) and LSMR-Tikhonov (5% and 20% noise levels) methods

Case no.	Noise levels (%)		
	0	5	20
1	46	20	42
2	52	21	51
3	40	20	33
4	39	34	43

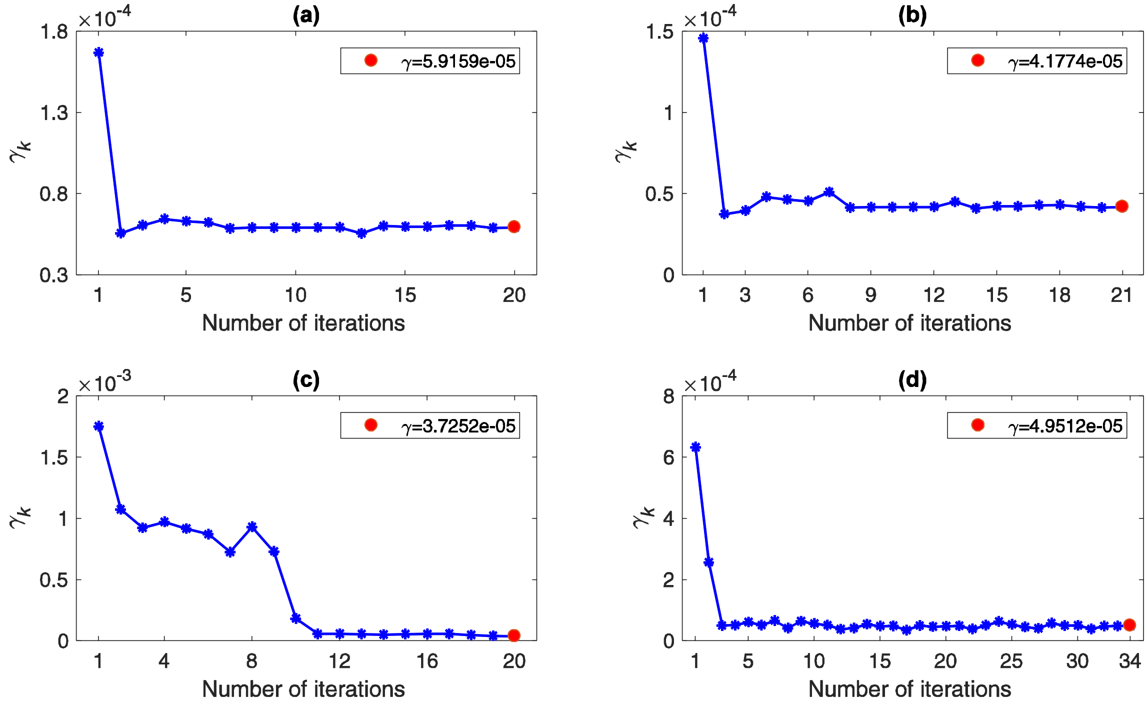

Fig. 2 The optimal regularization parameters under 5% noise level: **a** DC1, **b** DC2, **c** DC3, **d** DC4

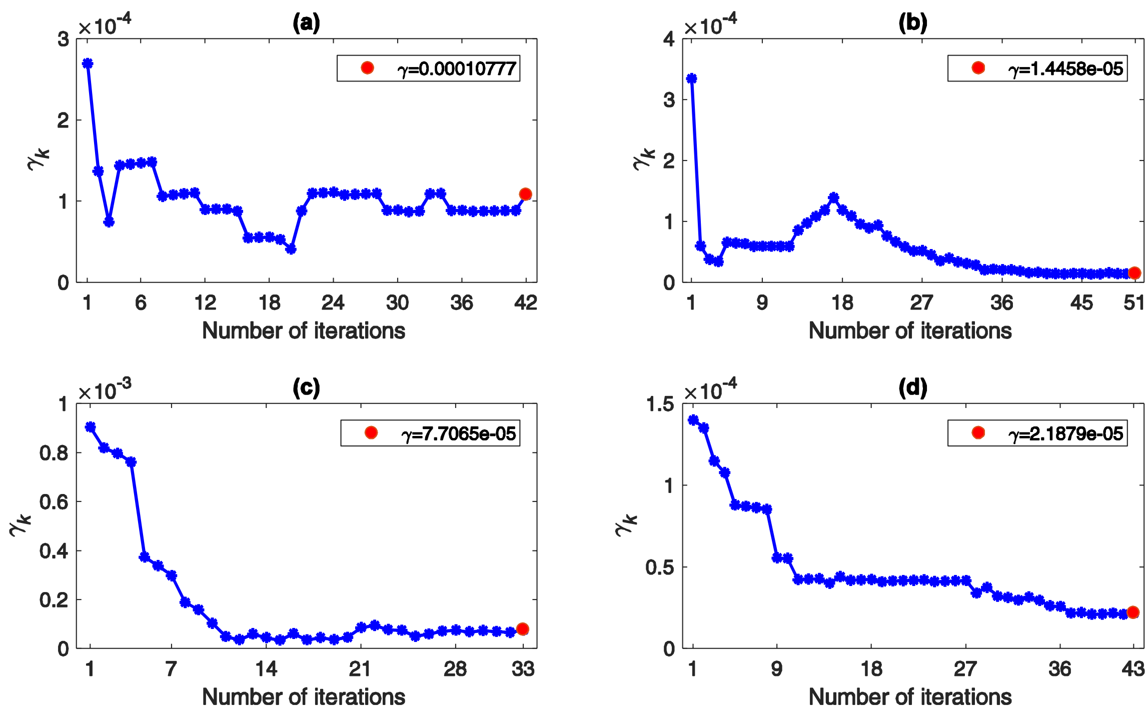

Fig. 3 The optimal regularization parameters under 20% noise level: **a** DC1, **b** DC2, **c** DC3, **d** DC4

The results of damage localization and quantification in all noise levels are shown in Figs. 4, 5 and 6. In these figures, the dashed red lines depict the threshold limits of the damage cases. As can be seen, the element 8 (E8) for the first and second damage cases (DC1-2) and the elements 5 and 15 (E5 and E15) for the third and fourth damage scenarios (DC3-4) are identified as the damage locations, because the damage values of these elements are more than the threshold

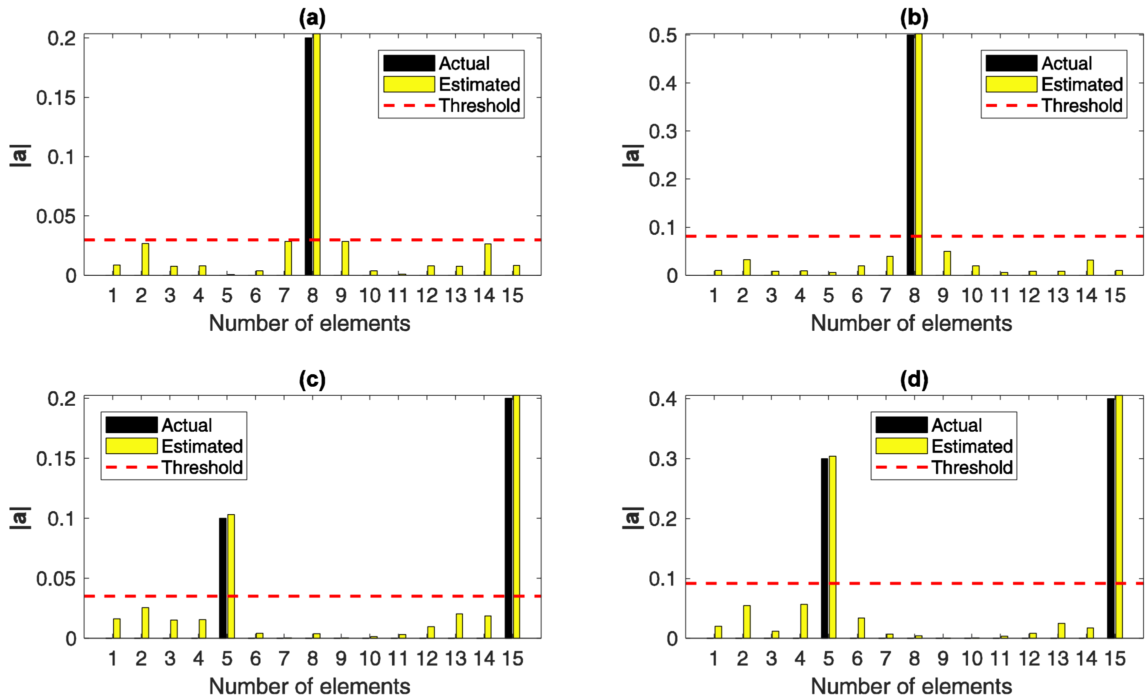

Fig. 4 Damage localization and quantification in the beam under the noise-free modal data: **a** DC1, **b** DC2, **c** DC3, **d** DC4

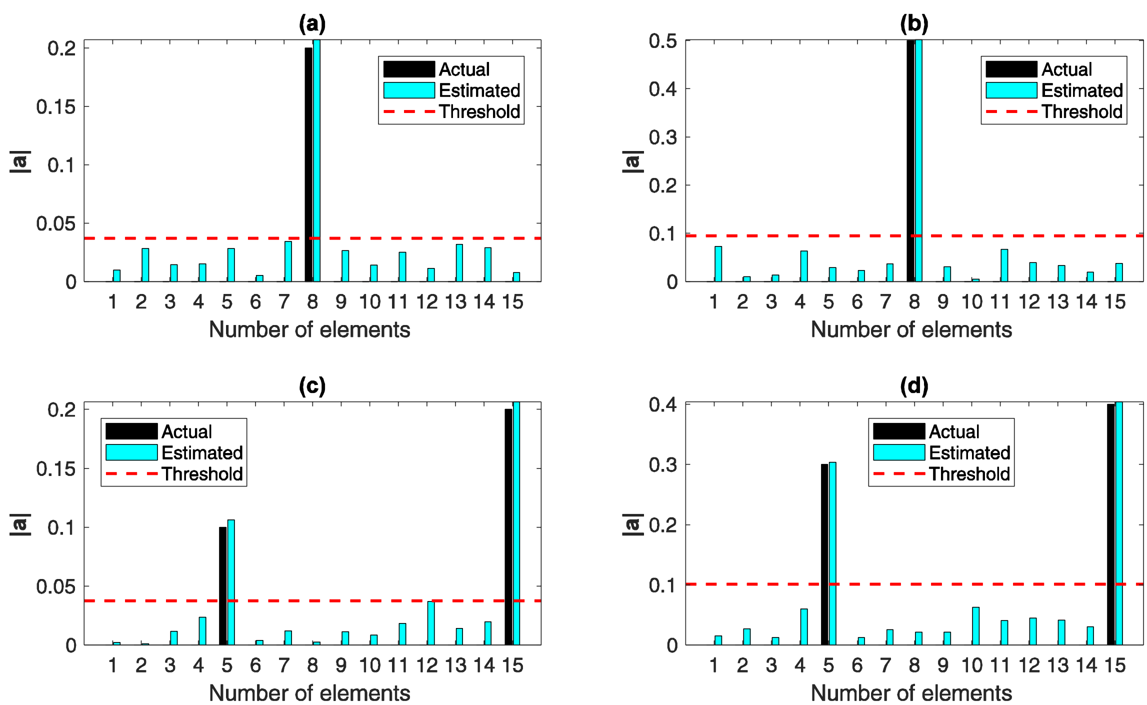

Fig. 5 Damage localization and quantification in the beam under 5% noise level: **a** DC1, **b** DC2, **c** DC3, **d** DC4

amounts. For the process of damage quantification, it is discerned that the values of |**a**| roughly correspond to the actual damage severities. This means that the proposed methods are accurately able to estimate the level of damage severity. Moreover, there are inconsiderable damage quantities of the undamaged elements, which can be neglected. Note that Fig. 4 belongs to the solution of the LS problem by using the LSMR method. It is apparent that under the noise-free modal

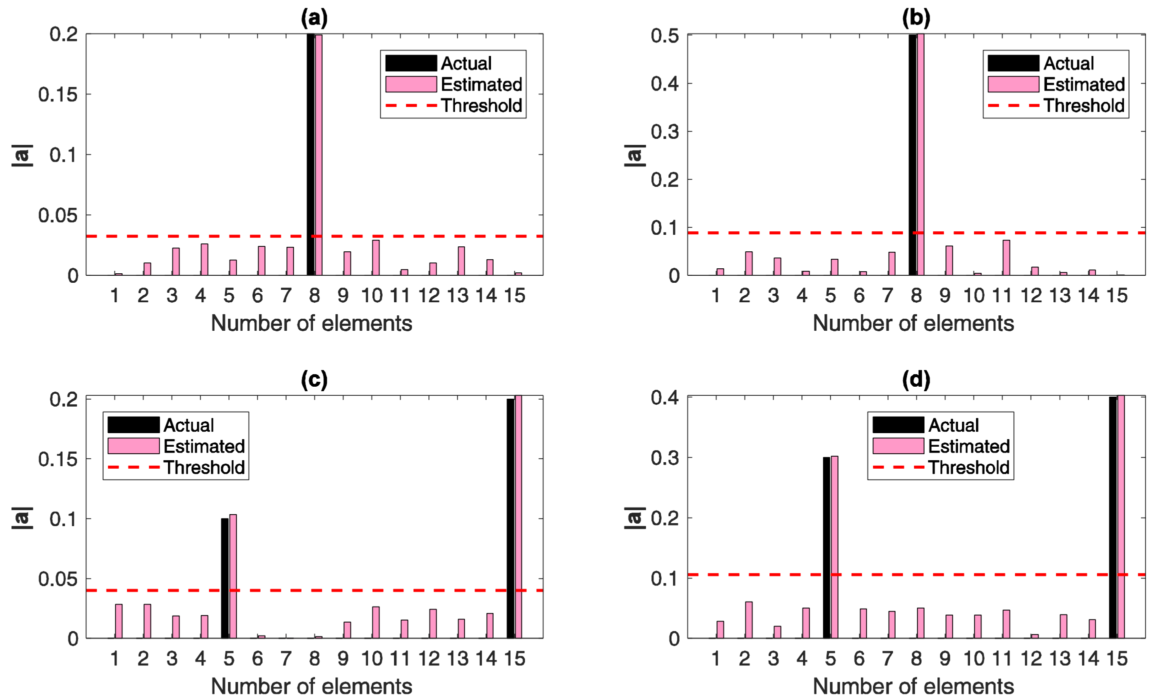

Fig. 6 Damage localization and quantification in the beam under 20% noise level: **a** DC1, **b** DC2, **c** DC3, **d** DC4

data, this iterative method yields reliable and satisfactory damage localization and quantification results. Although all observations in Figs. 4, 5 and 6 clearly demonstrate the accuracy and efficiency of the proposed methods for locating and quantifying the structural damages, it would be very appropriate to compare the enhanced and basic sensitivity functions of the modal flexibility. In this regard, Fig. 7 illustrates the relative errors (RE) between the estimated and actual damage values (severities) at the damaged elements in all cases.

As Fig. 7 shows, the relative errors obtained from the basic formulation are more than the enhanced function, particularly in DC2 and DC4, which include the relatively large damage severities. On the other hand, one can perceive that there are roughly inconsiderable relative errors (less than 4%) in the damage quantities gained by the improved sensitivity function. As a result, these conclusions demonstrate the superiority of the enhanced function over its basic formulation and confirm the positive effect of adding the expression ξ to the derivative of eigenvalue.

5.2 A simulated steel truss

For further assessment, a two-dimensional truss model is used to demonstrate the correctness and reliability of the enhanced and proposed methods. Figure 8 depicts this model along with the element numbers and dimensions. It consists of 25 elements and 21 DOFs. One assumes that the truss elements are comprised of steel with 200 GPa modulus of elasticity and 7850 kg/m^3 material density. The cross sections of the elements are invariant as presented in Table 3. Multiple damage scenarios are considered to simulate damaged conditions, which are originally available in [17]. The scenarios are based on reducing the stiffness of some elements as listed in Table 4.

The FE model of the truss containing the global mass and stiffness matrices are obtained by in-house MATLAB codes. Based on the model updating strategy for the damage detection process, this model is equivalent to an undamaged state. Hence, the analytical modal parameters are determined by the eigenvalue problem. For the damaged conditions, one supposes that the first five natural frequencies and mode shapes at a few DOFs including D2, D4, D6, D10, D15, and D19 are measurable. Four noise levels including 0%, 5%, 10%, and 20% are imposed on the measured modal parameters based on Eqs. (49) and (50). Similar to the previous numerical example, the modal displacements of the damaged conditions are scaled based on the mass-normalized analytical mode shapes. In addition, the SEREP technique is applied to expand the mass-normalized mode shapes of the damaged states. Table 5 lists the number of iterations needed to solve the damage equation. Likewise, the LSMR method is utilized to solve the LS problem in the noise-free data (0% noise level). For the noisy conditions, the GCV function $\bar{G}(k)$ for defining the stopping condition is applied to compute the number of iterations.

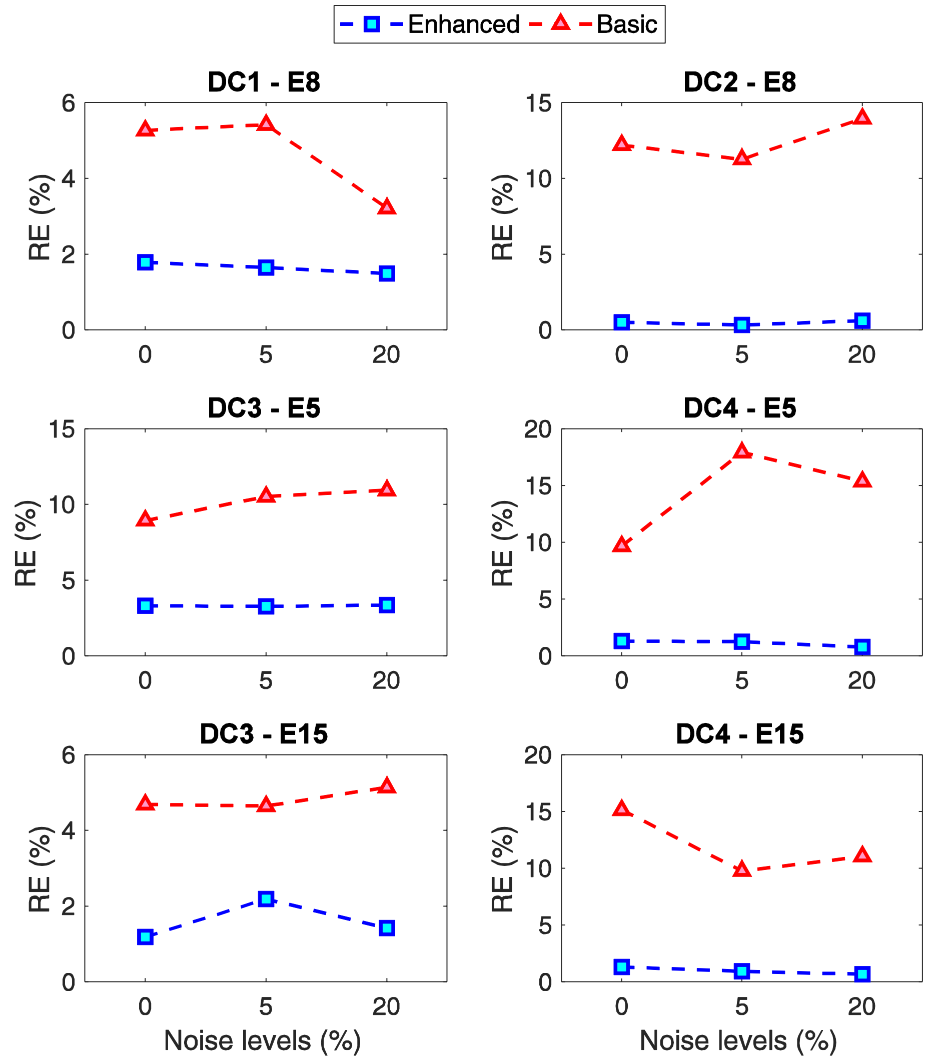

Fig. 7 Comparison of the basic and enhanced sensitivity functions of the modal flexibility in the beam model (*DC: Damage Case and E: Element*)

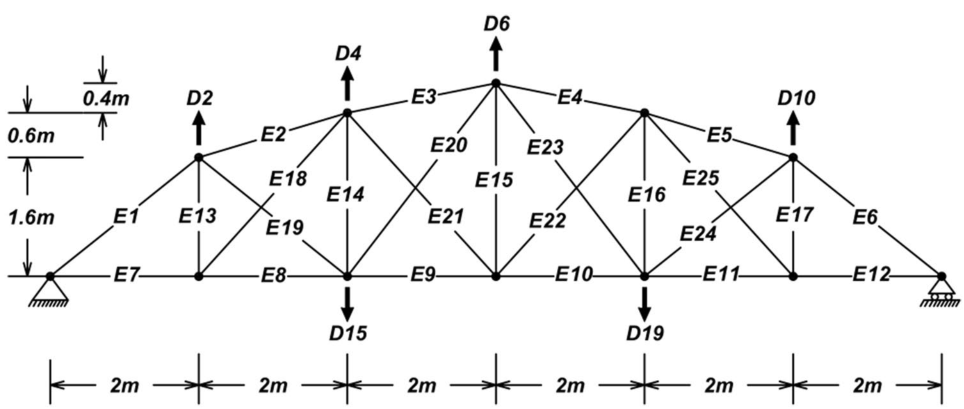

Fig. 8 The simulated truss model (*E: Element & D: Degree-of-freedom*)

Based on the GCV function for the determination of the optimal regularization parameter, Figs. 9 and 10 show the values of γ_k in the damage cases for the noisy conditions. The optimal regularization parameter required by the LSMR-Tikhonov method is obtained from $\hat{G}(\gamma_k)$ at the last iteration number, where is highlighted by the red circle.

The results of damage localization and quantification for DC1 and DC2 in all noise levels are shown in Figs. 11

Table 3 The invariant cross sections of the truss structure

Element no.	Area (m^2)
E1–E6	0.0018
E7–E12	0.0015
E13–E17	0.0010
E18–E25	0.0012

Table 4 Damage cases for the steel truss model

Case no.	Label	Damage location	Damage severity (%)
1	DC1	E4	15
		E11	30
2	DC2	E3	30
		E9	30
		E17	30

Table 5 The number of iterations for the LSMR (0% noise level) and LSMR-Tikhonov (5%, 10%, and 20% noise levels) methods

Case no.	Noise levels (%)			
	0	5	10	20
1	34	20	28	27
2	40	47	63	80

and 12, respectively. The dashed red arrows in these figures depict the threshold limits obtained from Eq. (51). Once again, the solution of the damage equation in the noise-free condition is carried out by the LSMR method as illustrated in Figs. 11a and 12a.

The damage locations are identified at elements whose absolute values of the damage vector exceed the threshold limits. As Fig. 11 reveals, the elements 4 and 11 are the damaged areas of the numerical truss model for DC1. Moreover, the elements 3, 9, and 17 are identified as the damage locations in DC2 as can be seen in Fig. 12. For the process of damage quantification, it is discerned that the results are reasonable and there are approximately no errors in the estimation of damage severities. Therefore, one can deduce that the enhanced and proposed methods have great abilities to locate and quantify multiple damages under the noise-free and noisy modal data.

Similar to the previous example, the superiority of the enhanced sensitivity function of the modal flexibility over the basic formulation is evaluated by comparing the relative errors in the damage severities of the damaged areas. Figure 13 shows the results of this comparative assessment for the first damage scenario. As expected, the enhanced sensitivity function gives more reliable and better results than the basic formulation. Based on Fig. 13, the relative errors of the enhanced sensitivity are roughly less than 2%, while there are considerable errors in the basic function. Therefore, the development of the eigenvalue derivative by adding the expression ξ leads to a more sensitive formulation to damage.

6 Conclusions

In this article, an improved sensitivity function regarding the modal flexibility and a hybrid solution method LSMR-Tikhonov were proposed to locate and quantify structural damage under the incomplete noisy modal data. A simply supported beam and a truss model were numerically simulated to verify the accuracy and reliability of the enhanced and proposed methods. The results in both of the numerical models demonstrated the accurate and precise damage localization and quantification. For locating the structural damage, a statistical threshold limit was used to increase

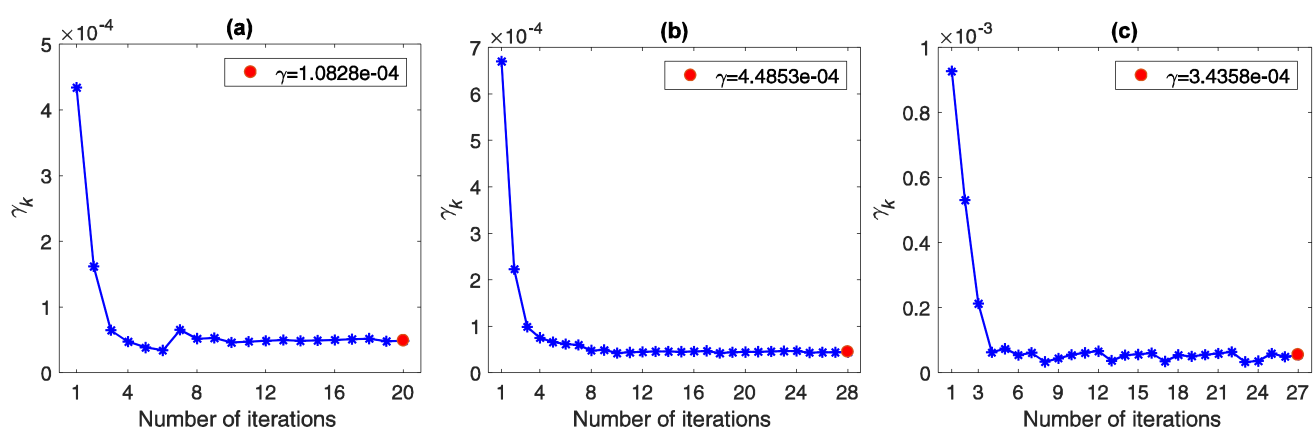

Fig. 9 The optimal regularization parameters for DC1: **a** 5% noise level, **b** 10% noise level, **c** 20% noise level

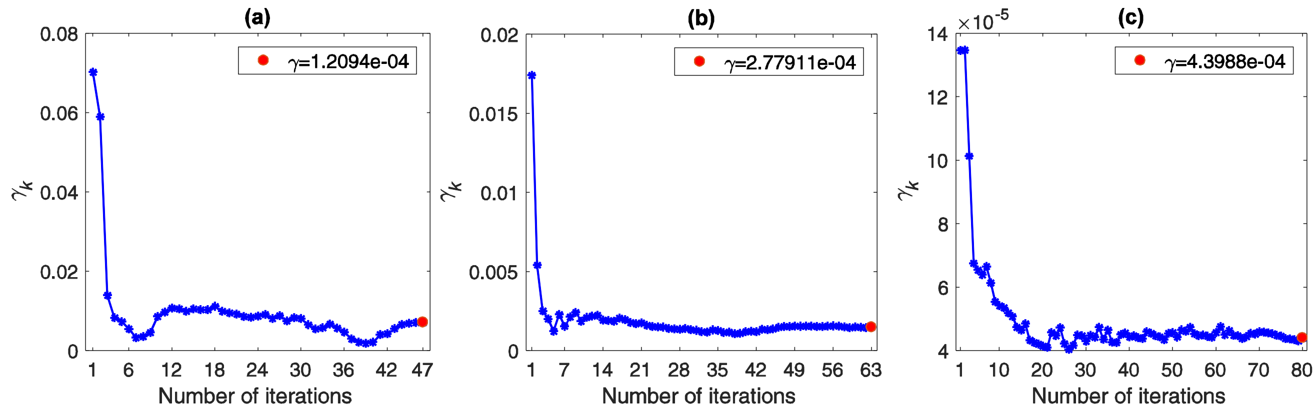

Fig. 10 The optimal regularization parameters for DC2: **a** 5% noise level, **b** 10% noise level, **c** 20% noise level

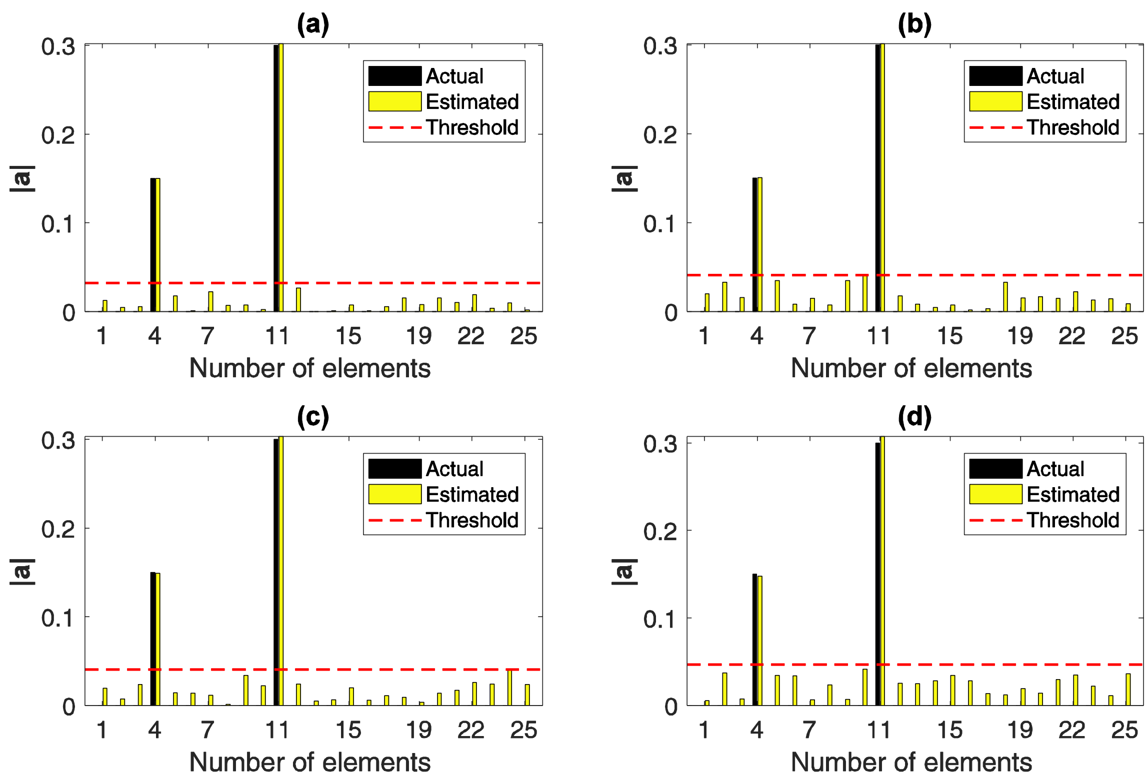

Fig. 11 Damage localization and quantification for DC1: **a** 0% noise level, **b** 5% noise level, **c** 10% noise level, **d** 20% noise level

the reliability of the damage localization. Each value of the damage vector larger than the threshold limit was indicative of the damage location. It was observed that the LSMR-Tikhonov method can efficiently solve any ill-posed LS problem by determining an optimal regularization parameter in an iterative manner. The comparative evaluations on the enhanced and basic sensitivity functions of the modal flexibility confirmed that the improved formulation is more sensitive to damage and provides better and more reliable results.

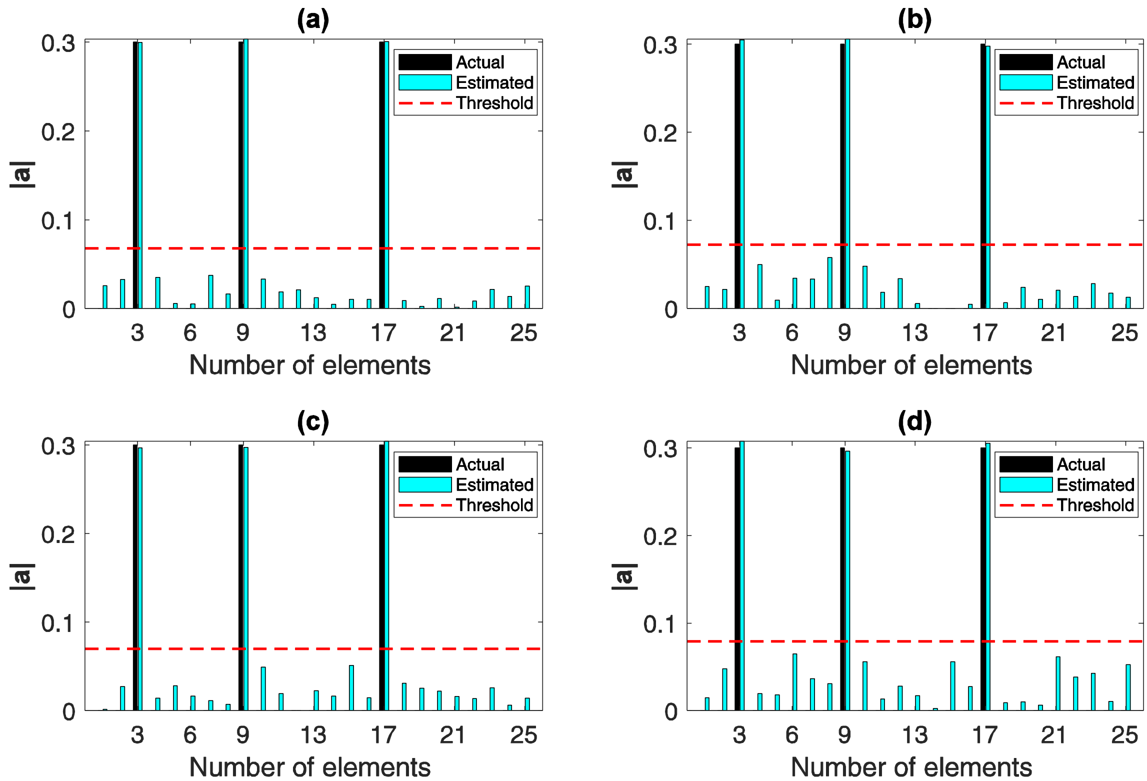

Fig. 12 Damage localization and quantification for DC2: **a** 0% noise level, **b** 5% noise level, **c** 10% noise level, **d** 20% noise level

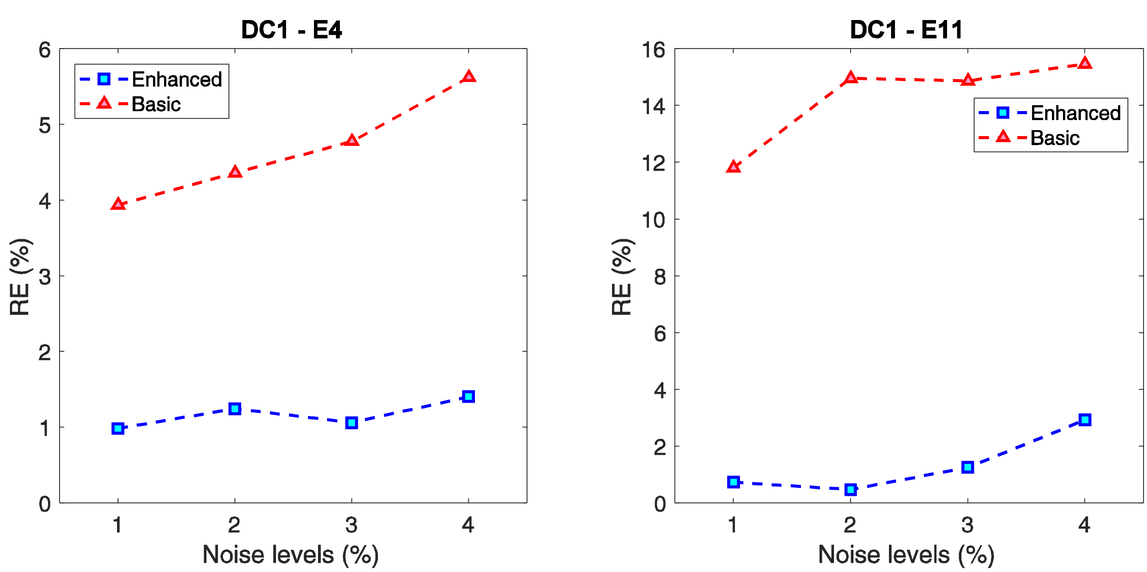

Fig. 13 Comparison of the basic and enhanced sensitivity functions of the modal flexibility in the truss model (*DC: Damage Case and E: Element*)

Compliance with ethical standards

Conflict of interest The authors declare that they have no conflict of interest.

References

1. Farrar CR, Worden K (2007) An introduction to structural health monitoring. Philos Trans R Soc A Math, Phys Eng Sci 365(1851):303–315
2. Farrar CR, Lieven NA (2007) Damage prognosis: the future of structural health monitoring. Philos Trans R Soc London A Math Phys Eng Sci 365(1851):623–632
3. Entezami A, Shariatmadar H, Sarmadi H (2017) Structural damage detection by a new iterative regularization method and an improved sensitivity function. J Sound Vib 399:285–307. https://doi.org/10.1016/j.jsv.2017.02.038
4. Lee E-T, Eun H-C (2019) Model-based damage detection using constraint forces at measurements. Eng Comput. https://doi.org/10.1007/s00366-019-00762-9
5. Ghasemi MR, Nobahari M, Shabakhty N (2018) Enhanced optimization-based structural damage detection method using modal strain energy and modal frequencies. Eng Comput 34(3):637–647. https://doi.org/10.1007/s00366-017-0563-5
6. Lee E-T, Eun H-C (2015) Damage identification of a frame structure model based on the response variation depending on additional mass. Eng Comput 31(4):737–747. https://doi.org/10.1007/s00366-014-0384-8
7. Ghiasi R, Fathnejat H, Torkzadeh P (2019) A three-stage damage detection method for large-scale space structures using forward substructuring approach and enhanced bat optimization algorithm. Eng Comput 35(3):857–874. https://doi.org/10.1007/s00366-018-0636-0
8. Sehgal S, Kumar H (2016) Structural dynamic model updating techniques: a state of the art review. Arch Comput Methods Eng 23(3):515–533
9. Sarmadi H, Karamodin A, Entezami A (2016) A new iterative model updating technique based on least squares minimal residual method using measured modal data. Appl Math Model 40(23):10323–10341. https://doi.org/10.1016/j.apm.2016.07.015
10. Entezami A, Shariatmadar H, Karamodin A (2019) Data-driven damage diagnosis under environmental and operational variability by novel statistical pattern recognition methods. Struct Health Monit 18(5–6):1416–1443. https://doi.org/10.1177/1475921718800306
11. Sarmadi H, Entezami A, Daneshvar Khorram M (2020) Energy-based damage localization under ambient vibration and non-stationary signals by ensemble empirical mode decomposition and Mahalanobis-squared distance. J Vib Control 26(11–12):1012–1027. https://doi.org/10.1177/1077546319891306
12. Sarmadi H, Karamodin A (2020) A novel anomaly detection method based on adaptive Mahalanobis-squared distance and one-class kNN rule for structural health monitoring under environmental effects. Mech Syst Signal Process 140:106495. https://doi.org/10.1016/j.ymssp.2019.106495
13. Thai D-K, Tu TM, Bui TQ, Bui T-T (2019) Gradient tree boosting machine learning on predicting the failure modes of the RC panels under impact loads. Eng Comput. https://doi.org/10.1007/s00366-019-00842-w
14. Mishra M, Bhatia AS, Maity D (2019) A comparative study of regression, neural network and neuro-fuzzy inference system for determining the compressive strength of brick–mortar masonry by fusing nondestructive testing data. Eng Comput. https://doi.org/10.1007/s00366-019-00810-4
15. Worden K, Farrar C, Manson G, Park G (2007) The fundamental axioms of structural health monitoring. Proc R Soc A Math Phys Eng Sci 463(2082):1639
16. Mottershead JE, Link M, Friswell MI (2011) The sensitivity method in finite element model updating: a tutorial. Mech Syst Signal Process 25(7):2275–2296. https://doi.org/10.1016/j.ymssp.2010.10.012
17. Rahai A, Bakhtiari-Nejad F, Esfandiari A (2007) Damage assessment of structure using incomplete measured mode shapes. Struct Control Health Monit 14(5):808–829. https://doi.org/10.1002/stc.183
18. Esfandiari A, Bakhtiari-Nejad F, Rahai A (2013) Theoretical and experimental structural damage diagnosis method using natural frequencies through an improved sensitivity equation. Int J Mech Sci 70:79–89. https://doi.org/10.1016/j.ijmecsci.2013.02.006
19. Zhao J, DeWolf JT (1999) Sensitivity study for vibrational parameters used in damage detection. J Struct Eng 125(4):410–416
20. Sung S, Koo K, Jung H (2014) Modal flexibility-based damage detection of cantilever beam-type structures using baseline modification. J Sound Vib 333(18):4123–4138
21. Bernal D, Gunes B (2004) Flexibility based approach for damage characterization: benchmark application. J Eng Mech 130(1):61–70
22. Duan Z, Yan G, Ou J, Spencer BF (2007) Damage detection in ambient vibration using proportional flexibility matrix with incomplete measured DOFs. Struct Control Health Monit 14(2):186–196
23. Zare Hosseinzadeh A, Ghodrati Amiri G, Seyed Razzaghi SA, Koo KY, Sung SH (2016) Structural damage detection using sparse sensors installation by optimization procedure based on the modal flexibility matrix. J Sound Vib 381((Supplement C)):65–82. https://doi.org/10.1016/j.jsv.2016.06.037
24. Lee E-T, Eun H-C (2017) Damage detection approach based on the second derivative of flexibility estimated from incomplete mode shape data. Appl Math Model 44:602–613. https://doi.org/10.1016/j.apm.2017.02.014
25. Yang Q (2009) A mixed sensitivity method for structural damage detection. Int J Numer Methods Biomed Eng 25(4):381–389
26. Li J, Wu B, Zeng Q, Lim CW (2010) A generalized flexibility matrix based approach for structural damage detection. J Sound Vib 329(22):4583–4587
27. Yan W-J, Ren W-X (2014) Closed-form modal flexibility sensitivity and its application to structural damage detection without modal truncation error. J Vib Control 20(12):1816–1830
28. Titurus B, Friswell M (2008) Regularization in model updating. Int J Numer Meth Eng 75(4):440–478
29. Saeedi A, Pourgholi R (2017) Application of quintic B-splines collocation method for solving inverse Rosenau equation with Dirichlet's boundary conditions. Eng Comput 33(3):335–348. https://doi.org/10.1007/s00366-017-0512-3
30. Pourgholi R, Tabasi SH, Zeidabadi H (2018) Numerical techniques for solving system of nonlinear inverse problem. Eng Comput 34(3):487–502. https://doi.org/10.1007/s00366-017-0554-6
31. Saeedi A, Foadian S, Pourgholi R (2019) Applications of two numerical methods for solving inverse Benjamin–Bona–Mahony–Burgers equation. Eng Comput. https://doi.org/10.1007/s00366-019-00775-4
32. Wang L, Xie Y, Wu Z, Du Y, He K (2019) A new fast convergent iteration regularization method. Eng Comput 35(1):127–138. https://doi.org/10.1007/s00366-018-0588-4
33. Weber B, Paultre P, Proulx J (2009) Consistent regularization of nonlinear model updating for damage identification. Mech Syst Signal Process 23(6):1965–1985

34. Hou R, Xia Y, Zhou X (2018) Structural damage detection based on l_1 regularization using natural frequencies and mode shapes. Struct Control Health Monit 25(3):e2107. https://doi.org/10.1002/stc.2107
35. Grip N, Sabourova N, Tu Y (2017) Sensitivity-based model updating for structural damage identification using total variation regularization. Mech Syst Signal Processing 84(Part A):365–383. https://doi.org/10.1016/j.ymssp.2016.07.012
36. O'Callahan JC, Avitabile P, Riemer R (1989) System equivalent reduction expansion process. Paper presented at the Seventh international modal analysis conference, Las Vegas, Nevada, USA
37. Golub G, Kahan W (1965) Calculating the singular values and pseudo-inverse of a matrix. J Soc Industr Appl Math Ser B Numer Anal 2(2):205–224. https://doi.org/10.1137/0702016
38. Fox R, Kapoor M (1968) Rates of change of eigenvalues and eigenvectors. AIAA J 6(12):2426–2429
39. Chung J, Palmer K (2015) A hybrid LSMR algorithm for large-scale Tikhonov regularization. SIAM J Sci Comput 37(5):S562–S580

Publisher's Note Springer Nature remains neutral with regard to jurisdictional claims in published maps and institutional affiliations.